Circulation and Fluxes in the North Atlantic between Greenland and Ireland

SHELDON BACON

Southampton Oceanography Centre, Southampton, United Kingdom

(Manuscript received 6 September 1995, in final form 17 January 1996)

ABSTRACT

Quasi-meridional flux estimates for volume, heat, and freshwater, with computed errors, in the region of the subpolar gyre of the North Atlantic between Cape Farewell and Ireland between 53° and 60°N are presented. The dataset consists of three approximately 500-km-sided boxes of CTD stations collected as the U.K. Control Volume Experiment during summer 1991 on the RRS *Charles Darwin*, supplemented by stations from the International Geophysical Year surveys of the R/V *Anton Dohrn* to represent the East Greenland Current (EGC), and justification is given for their use. The circulation is determined by an inverse method applied to the boxes of the survey, with in situ current measurements from a vessel-mounted acoustic Doppler current profiler forming an estimate of the strength of the EGC. Climatological wind stress data are used to estimate Ekman fluxes. The principal results are the determination of the poleward heat flux across the survey region as 0.28 ± 0.06 PW, and of the freshwater gain by the Arctic as $0.17 \pm 0.06 \times 10^6$ m^3 s^{-1}. A quantified circulation scheme for the part of the subpolar gyre covered by the survey is presented, for which the upper circulation agrees with that of previous authors (within the errors of the estimates), but the deep circulation, particularly the Denmark Strait overflow, appears significantly weaker than previous estimates.

1. Introduction

In this paper, we generate a circulation scheme for the waters of the northeast Atlantic between Greenland and the European continental shelf, from which we derive estimates of total (quasi-meridional) fluxes of volume, heat, and freshwater. This analysis provides a modern view of part of the Atlantic circulation that has long been reliant on the International Geophysical Year (IGY) data. Here we present synoptic near-zonal sections with reliable current, flux and error determinations at these latitudes. We will not review previous work on circulation in the subpolar gyre, meaning the region encompassed by the northern overflows south of the Greenland–Iceland–Scotland sill, the North Atlantic Current north of about 50°N, the East Greenland Current, and related features; rather, in view of the piecemeal nature of existing flux estimates in this region, the reader is referred to the fine recent reviews of North Atlantic circulation by Schmitz and McCartney (1993) and Reid (1994).

The U.K. Control Volume Experiment (CONVEX-91) data have been presented in Read and Gould (1992) in the context of climate change, and also in a companion paper to this one (Bacon 1994, hereafter B94), to which the reader is referred for a description of the CTD and ADCP (acoustic Doppler current profiler) data, the details of the inverse method (due to Wunsch l978), and the B94 technique for comparing inversion solutions with ADCP-derived solution estimates. Some information is repeated here for convenience. The CONVEX-91 cruise took place between 1 August and 4 September 1991 on the RRS *Charles Darwin*, between Ireland and Cape Farewell. The cruise program is described in Gould (1992). Station positions and bathymetry are shown in Fig. 1, with the station sequence indicated by highlighting selected stations. A total of 96 numbered stations were occupied, of which numbers 40 and 79–82 were repeats and are not included here. Also, bad weather prevented a cast from being made at station 8. The three boxes are named west, center, and east. Reference will also be made to the four principal sections into which the data fall: south section (the continuous line from stations 49 to 1); north section (the continuous line from stations 49 to 48 to 96); and west and east sections (31 to 67, and 20 to 10, respectively). See B94 for details of the removal of the M_2 tide from the ADCP data, all subsequent references to which imply detided data.

2. Fabrication of East Greenland Current data

First, we address the absence of the East Greenland Current (EGC) from the CONVEX data. Foul weather prevented work in the final 70 km of sections whose total length coast-to-coast was over 2500 km; the last

Corresponding author address: Dr. Sheldon Bacon, James Rennell Division, Southampton Oceanography Centre, Empress Dock, Southampton SO14 3ZH, United Kingdom.
E-mail: S.Bacon@soc.soton.ac.uk

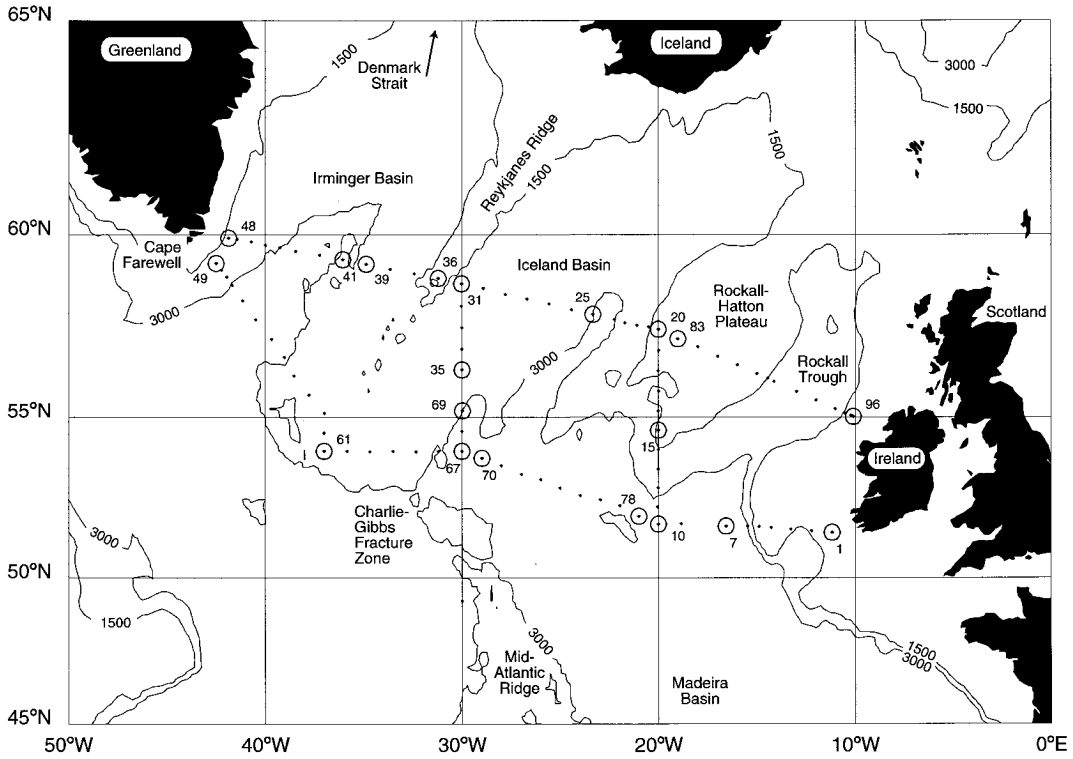

FIG. 1. CONVEX station positions with selected positions highlighted.

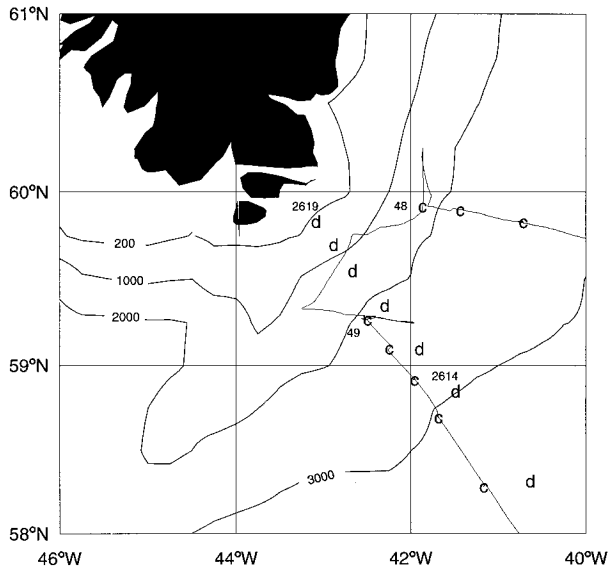

FIG. 2. Magnified view of western end of CONVEX area. The letter ''c'' indicates CONVEX station positions (as in Fig. 1), and the letter ''d'' indicates R/V *Anton Dohrn* station positions. The six of these latter employed in the text are numbers 2614 (southeastern) to 2619 (northwestern). The faint continuous line joining the CONVEX stations is the track of the RRS *Charles Darwin.*

westward station in the north section (48, on 17 August) and the subsequent first eastward station in the south section (49, on 19 August) were both just outside the EGC by about 10–15 km. This was determined by examination of thermosalinograph data (not shown here), which shows the very sharp salinity front at the eastern edge of the EGC. However, useful measurements of the strength of the EGC were acquired: During the two days between stations 48 and 49, and also for 20 hours between stations 47 and 48, the ship was mainly hove-to and collecting good ADCP data. In this section we will show that a reliable estimate of the geostrophic reference current can be made with these data, and that in combination with historical data to provide the vertical current shear, a useful (if hybrid) EGC can be included in this study. Also, the salt flux between the westernmost station and the coast will be inspected to see if the extreme salinities encountered near the coast might be significant.

The logical choice of historical data was the western part of the IGY (section 4) (summer), made on the R/V *Anton Dohrn* in 1958 (Dietrich 1969) because the tracks of the CONVEX south section and IGY section 4 are nearly coincident in the Irminger Basin. Accordingly, six IGY stations, numbers 2614–2619, were used; their positions, with CONVEX stations, detailed CONVEX ship track, and bathymetry are shown in Fig. 2. The pairs 2614–2615 and 2615–2616 will be compared with CONVEX, and geostrophic profiles and associated properties of the three pairs 2616–2619 will be used to represent the EGC contiguously with the CONVEX sections.

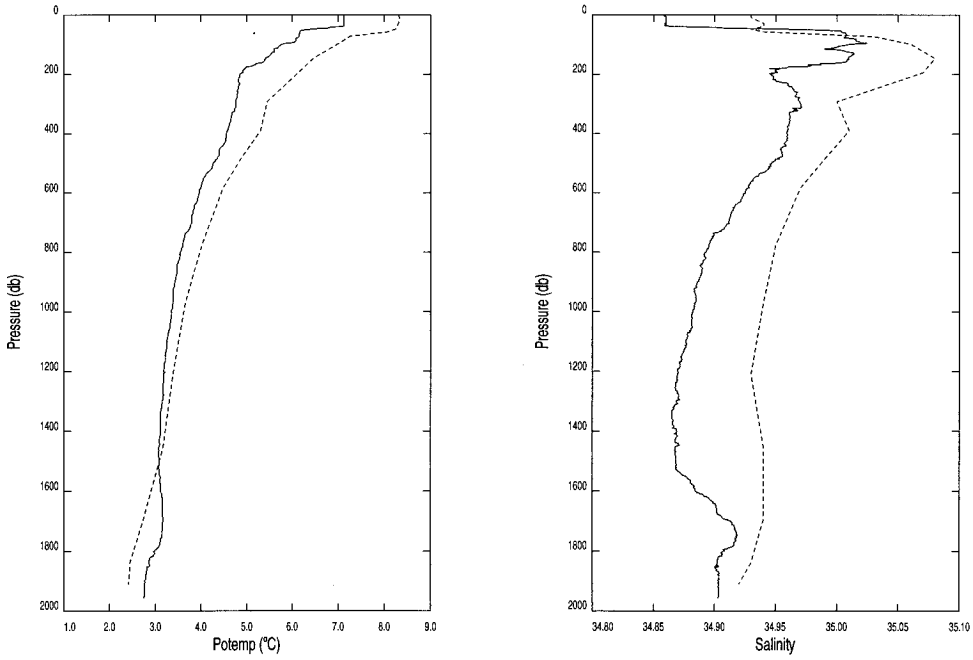

FIG. 3. Comparison of potential temperature profiles and salinity profiles at CONVEX station 49 and R/V *Anton Dohrn* station 2616. CONVEX profiles are full lines, *Anton Dohrn* profiles faint lines.

We want to compare the IGY and CONVEX vertical current shears. First, it is noted that there have been large changes in water properties. Based on potential temperature and salinity at stations 49 and 2616 (Fig. 3), which are close together and separated ~15 km in a direction parallel to the isobaths, a cooling and freshening of the water occurred (cf. Read and Gould 1992), the magnitudes of which greatly exceed the dominant measurement accuracy, which for IGY salinity was ~0.01 and for IGY temperature ~0.01°C. Two pairs of stations are needed to proceed with the comparison, so 49 and 2616 are taken as ''matched''; the simplest way to produce a CONVEX ''station'' matching 2615 is to average 50 and 51. Then geostrophic profiles were calculated, referenced to 1000 m, for the IGY stations (2615 and 2616) and for the CONVEX stations (49 and ''50–51''). The resulting profiles are shown in Fig. 4a. The vertical shears are similar above 1000 m and different below 1000 m, which we discuss later. Although properties have changed, the upper-ocean horizontal density gradients have not. This comparison is repeated for CONVEX stations ''50–51'' and 52, and IGY stations 2614 and 2615; the resulting shear profiles are shown in Fig. 4b. We will need estimates of the property changes; they are shown in Fig. 5. The CONVEX data are cooler (−0.58°C) and fresher (−0.038 psu) than the IGY data, where the differences are calculated as averages above 1000 m.

We turn now to the ADCP data. The ship's track near Cape Farewell is shown in Fig. 2, where it can be seen that in drifting while hove-to, the ship covered isobaths at depths of all but the innermost station pair (2618–2619). Estimation of the geostrophic reference current as the difference between ADCP current and bottom-referenced geostrophic current at a fixed depth will be attempted. The mid (2617–2618) profile terminates around 170-m depth, and it was argued in B94 that rotational currents do not extend to 100-m depth during CONVEX. Therefore, we will use data at 100 m to estimate reference currents. Figure 6 shows 15-min mean absolute current vectors at 100-m depth for % good $>$ 50% and for ship speeds through the water less than 2.5 m s^{-1} near Cape Farewell. The current is quite steady, with mean magnitude 30.9 cm s^{-1} (std dev 11.5 cm s^{-1}) and direction 227° (std dev 30°). The direction is nearly perpendicular to the sections. By comparing the three IGY profiles, referenced to zero at the bottom, with the above figure for the current at 100 m, the following reference currents of 20 cm s^{-1} (inner), 29 cm s^{-1} (mid), and 15 cm s^{-1} (outer) are estimated. We have assumed that the mean ADCP current at 100 m can be applied to the inner, shallowest station pair.

The total southward volume flux in the three station pairs comprising the EGC is then 15.0 Sv (Sv $\equiv 10^6$ m^3 s^{-1}), of which 4.2 Sv derive from the velocity shears referenced to zero at the bottom. Potential temperatures and salinities are adjusted by constant offsets to bring the IGY values in line with the modern data. No significant differences resulted from replacing the mean offsets with vertically graduated ones reflecting the difference profiles, Fig. 5.

Now the inshore salt flux, between *Anton Dohrn* station 2619 and the coast is considered. This estimate will be crude because of the paucity of data. The cross-

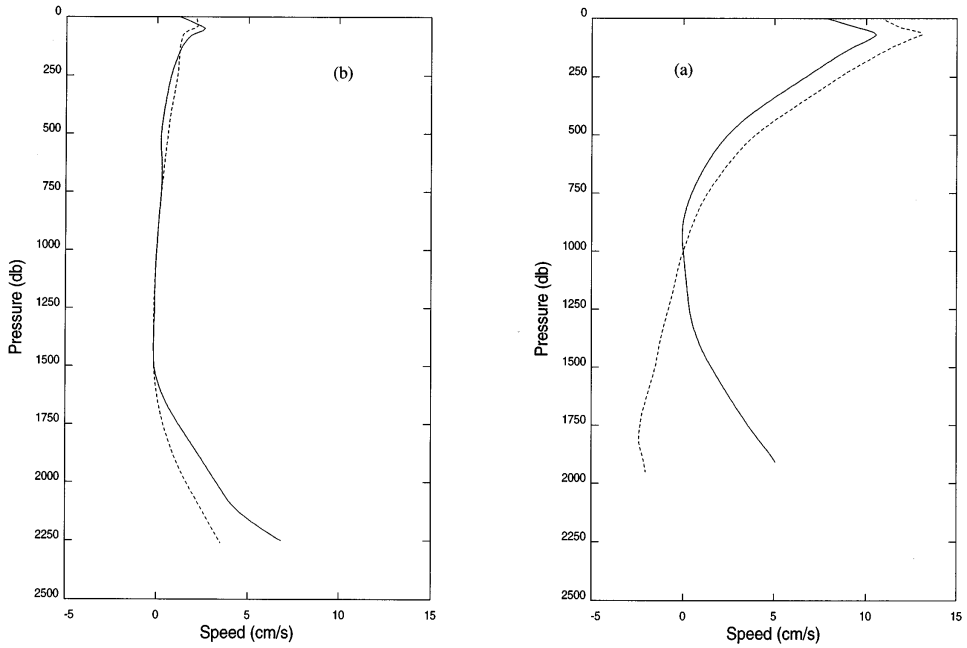

FIG. 4. Comparison of geostrophic velocity profiles, referenced to zero at 1000 m, formed (a) from *Anton Dohrn* stations 2615 and 2616 and from CONVEX stations 49 and ''50–51'' (see text for explanation). CONVEX profiles are full lines, *Anton Dohrn* profiles faint lines, and (b) from *Anton Dohrn* stations 2614 and 2615 and CONVEX stations ''50–51'' and 52.

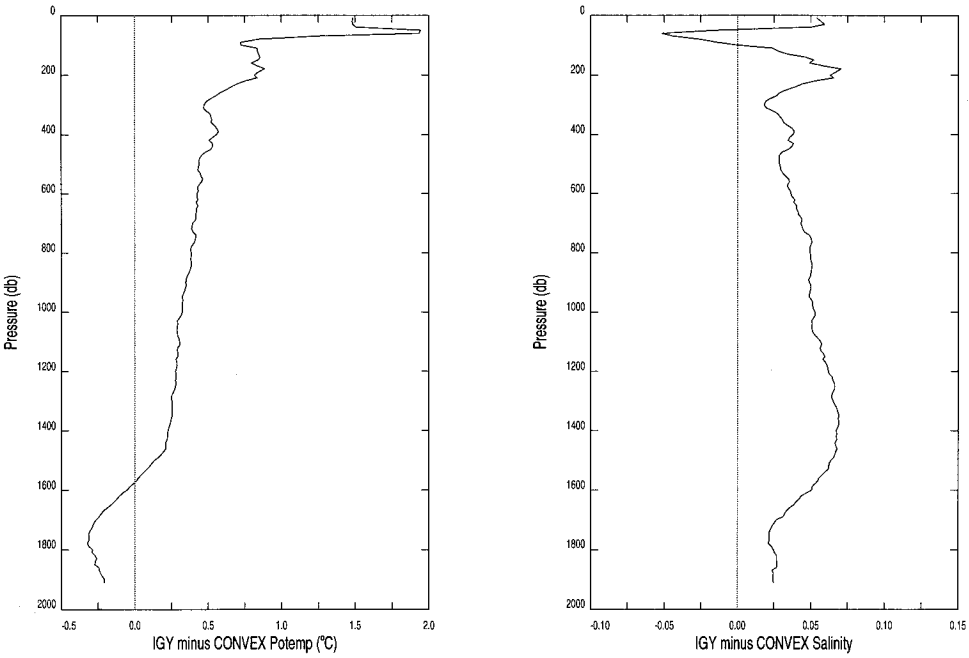

FIG. 5. Potential temperature and salinity difference profiles. Differences (*Anton Dohrn* minus CONVEX) are calculated between mean property profiles formed from *Anton Dohrn* stations 2615 and 2616, and from CONVEX stations 49 and ''50–51'' (see text for explanation). Both profiles were averaged/interpolated to 10-m vertical resolution.

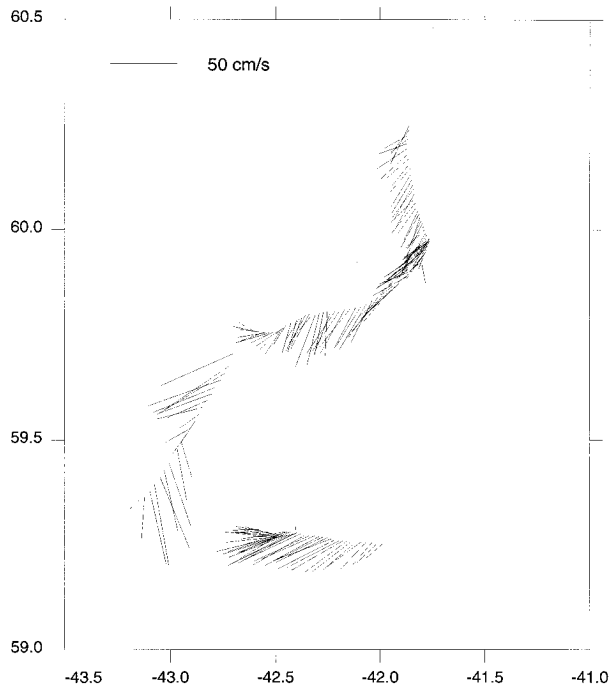

FIG. 6. ADCP currents in the vicinity of the East Greenland Current. Data shown are of greater than 50% good, for ship speed less than 2.5 m s^{-1}, at 100-m depth. All good data after and excluding station 47 and before and excluding station 50 are shown.

sectional area between 2619 and the beach is taken to be triangular such that the offshore depth is 170 m and the offshore distance is 20 km, resulting in an area of 1.7×10^6 m^2. We assume the currents to be barotropic and decreasing linearly from 40 cm s^{-1} at 2619 to zero at the coast, and a mean salinity profile from 2619, salinity ~32.5 psu, is used from which the salinity anomaly (difference from the section mean) is approximately −2.5 psu. Thus, we estimate the inshore volume flux to be 0.45 Sv and the resulting salt flux to be 1.13 Sv psu, which is quite large. It is also probably an underestimate since, as one approaches the coast, one approaches a source of the freshening of the EGC, that is, local glacial meltwater runoff. It is difficult to estimate an error for what is itself a crude estimate, but an attempt is made through examination of the deviation of the data from the assumptions. The baroclinic component of the velocity profile at 2619 has a velocity ''error'' of ±20 cm s^{-1}. The salinity profile at 2619 has a salinity error of ±1 psu. In combination the inshore salt flux error is about ±1 Sv psu.

3. Preferred flow field

a. Derivation

The preferred flow field is derived after the manner of Bryden and Hall (1980), whereby the circulation is divided into three components: (i) the western boundary current (the EGC, described above in section 2), (ii) the Ekman flux, and (iii) the interior geostrophic circulation. The total net volume flux is constrained to a fixed value (zero). First, this constraint is examined.

There are three areas where oceanic water can enter or leave the Arctic: (i) through the Bering Strait, where the transport has been reported by Coachman and Aagaard (1989) and Roach et al. (1995); (ii) through the Canadian Archipelago, reported by Fissel et al. (1988); and (iii) between Greenland and Europe, as ice as well as water. The large terms are the Bering Strait inflow to the Arctic (about 1 Sv) and the Canadian Archipelago Throughflow, which exports water from the Arctic at about 1–2 Sv. Therefore, the net flow between Greenland and Europe must be small: probably 0 ± 1 Sv. The smaller terms will be considered in section 5.

Climatological values of wind stress due to Hellerman and Rosenstein (1983) are used to estimate the cross-track Ekman fluxes of volume, temperature, and salt. The Ekman volume fluxes are southward of magnitude 2.0 Sv (south section) and 1.0 Sv (north section). The values of potential temperature and salinity at 10 m are chosen for determination of Ekman contributions to property fluxes. Their track-length-weighted mean values are, for potential temperature, 12.130°C (south) and 12.249°C (north); and for salinity, 34.884 psu (south) and 34.994 psu (north).

The interior geostrophic circulation is derived from the CONVEX hydrographic survey data, and here the inverse method used is described. There are three connected boxes of CTD stations. Note that the western box is closed across stations 48–49 and is not made to connect to Greenland. The criterion for selection of the ''first guess'' level of no motion for the geostrophic base state is minimum volume flux divergence, the application of which results in identification of the level σ_2 = 36.93, and which produces small (0–2 Sv) net outflows from all three boxes. The water column over the survey region is divided into five layers by application of the optimization technique described in Bacon (1997, manuscript submitted to *J. Atmos. Oceanic Technol.*); these layers are defined by the sea surface, σ_0 = 27.425, σ_2 = 36.873, 36.944, 37.024, and the bottom, Fig. 7. The selected EGC stations (excluding 2616, which is in the same position as CONVEX 49) are also included in the figure, with densities as calculated from their original properties. The inverse model is that of Wunsch (1978) for determining geostrophic reference currents, with the modification of B94 for selection of solution degree, and consists of constraints in the form of horizontal flux conservation equations written for each layer and for each box; the conservation equations are coupled at the east and west sections. Volume flux and salt flux conservation are required in all layers; temperature flux conservation is required in all layers except the top one. The temperature and salinity fields are shown in Figs. 8 and 9. A total of 42 constraints results, and using B94, we select solution degree 6, which is shown in Fig. 10.

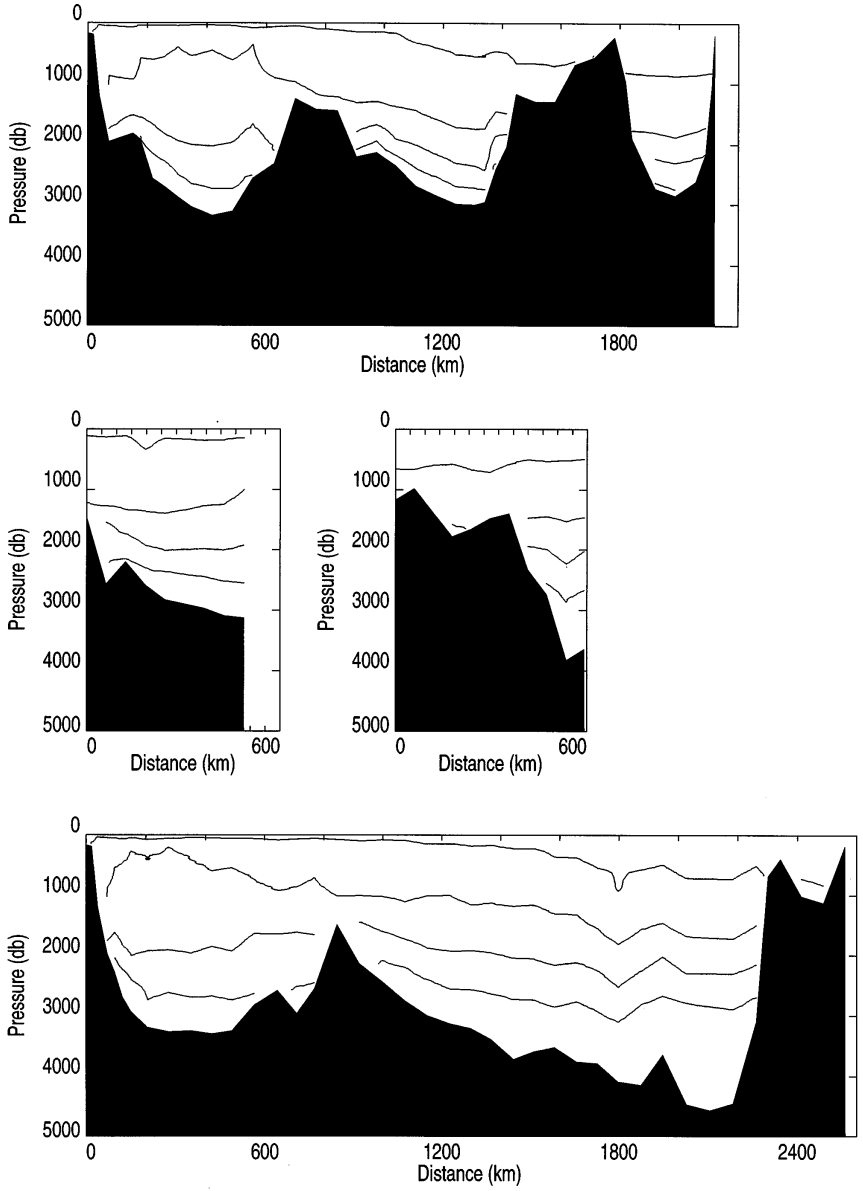

FIG. 7. Density levels for the 5-layer optimal configuration (σ_0 = 27.425, σ_2 = 36.873, 36.944, 37.024). The top and bottom panels are the north and south sections, respectively, both with west to the left. The center panels are the west (left) and east (right) sections, both with north to the left.

It is not possible to accurately determine two components of the flux: (i) the southward reference currents in the two westernmost CONVEX pairs on both north and south sections and (ii) the northward reference currents in the North Atlantic Current, again on both north and south sections. However, it is possible to place limits on their magnitudes, as described in the next section.

b. Limiting fluxes

That some elements of the circulation are not accurately determined stems from the observation that the Denmark Strait overflow (DSO) appears very weak in our data: 3–4 Sv, from the circulation components assembled in section 3a above. We note that the top of layer 4 (σ_2 = 36.944, the top of our DSO) is nearly exactly coincident with that used by Dickson and Brown (1994, hereafter DB94) of σ_0 = 27.8 to delineate the division between the deep western boundary current (DWBC) and overlying waters. We compare our weak DSO with the estimate of its strength from the measurements made by Clarke (1984) in 1978, which were used by DB94 to derive a transport of 13.3 Sv southward. Thus, there is a ''shortfall'' of ~10 Sv that must be reconciled. First we will inspect the barotropic and then the baroclinic

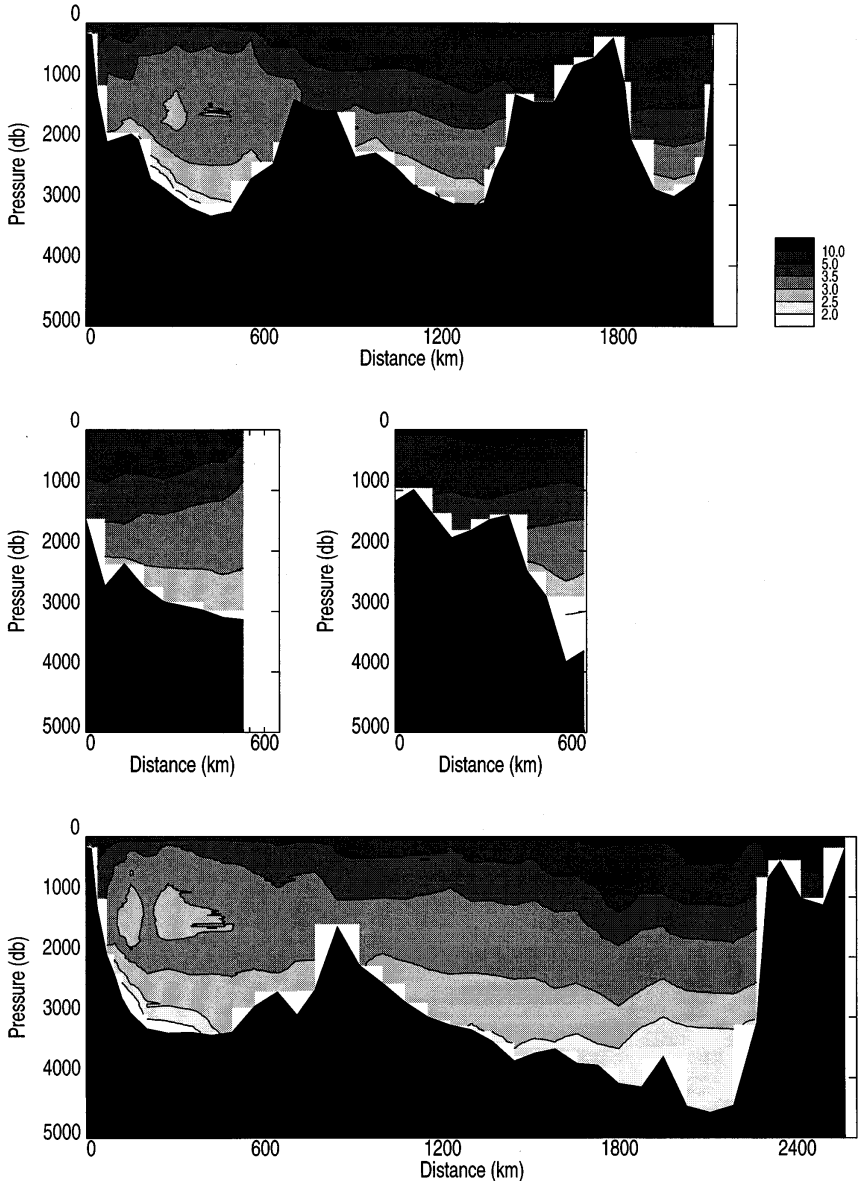

FIG. 8. Potential temperature (θ). The top and bottom panels are the north and south sections respectively, both with west to the left. The center panels are the west (left) and east (right) sections, both with north to the left.

currents in the area to determine whether any differences can be identified.

Comparison of Clarke's (1984, his Fig. 6) current field near Greenland with that of CONVEX shows that in the water column over the approximate depth range of the core of the DSO (1800–3000 m), there is a mean current difference whereby Clarke's currents are greater than CONVEX by 5–10 cm s^{-1}. The present ADCP offsets (mean differences between ADCP currents and bottom-referenced geostrophic profiles: Fig. 11) in the same area at the westernmost two station pairs (both north and south sections) are of average magnitude 11 cm s^{-1} and are nearly parallel. The overall mean offset is near zero (-0.8 cm s^{-1}) with large standard deviation (8 cm s^{-1}), and B94 showed that the background amplitude of ageostrophic transients was 5–8 cm s^{-1}, so these measurements are marginally significant. By imposing additional reference currents of 11 cm s^{-1} (southward) in the westernmost two station pairs in the north and south sections, an extra net southward flux of 12.5 Sv is obtained, of which 3.5 Sv goes below $\sigma_2 = 36.944$, so that the DSO becomes ~7 Sv. The net southward flux off Greenland, between the coast and the center of the Irminger Basin, is increased from 20 to 32.5 Sv. It is shown later that the southward flux off Greenland is a useful diagnostic of the strength of the general subpolar

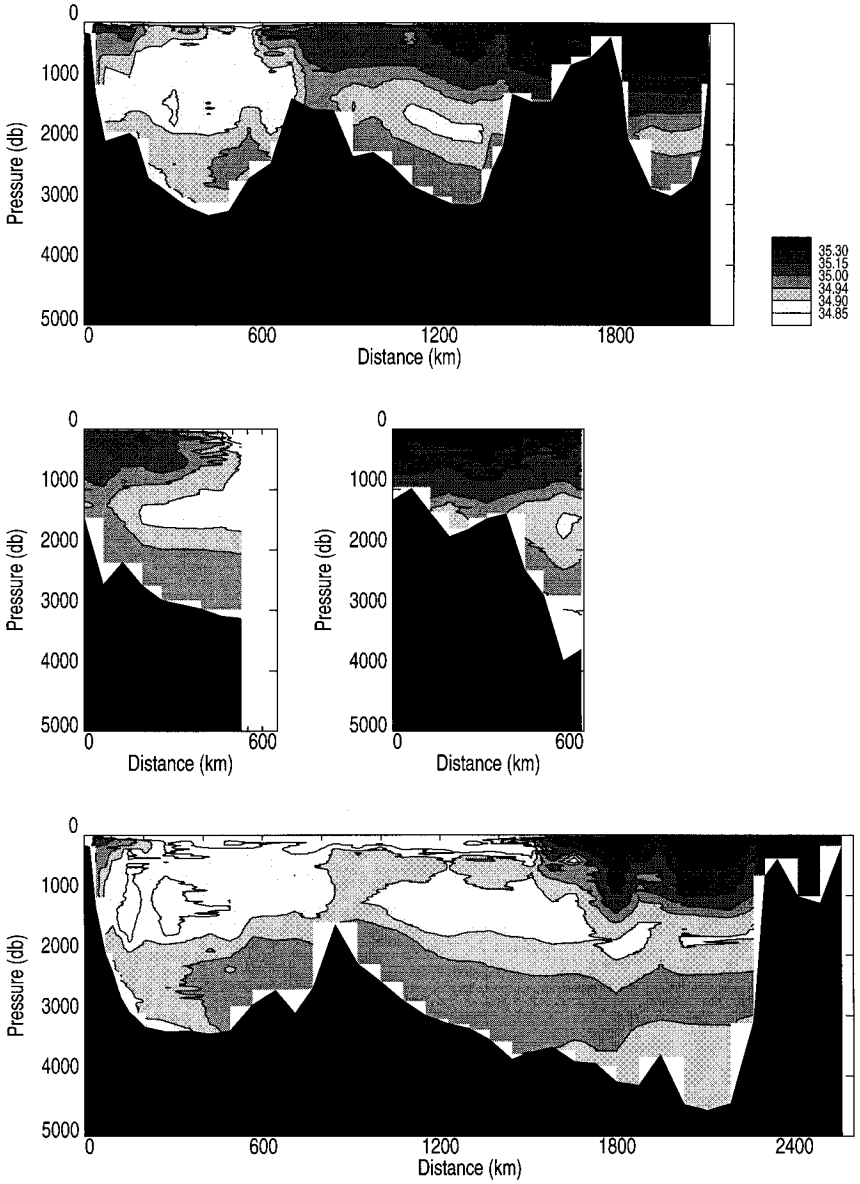

FIG. 9. Salinity. The top and bottom panels are the north and south sections respectively, both with west to the left. The center panels are the west (left) and east (right) sections, both with north to the left.

circulation. Note here that in order to obtain a DSO of 13.3 Sv by barotropic adjustment, the general circulation would need to be increased from 20 to ~60 Sv, which is excessive.

Has there been a significant baroclinic change? If (Fig. 4) we match the very similar upper velocity shears of the CONVEX and IGY data, the deep shears in the later data are much reduced compared with the earlier data. To reinstate this ''lost'' shear, the depth range of 1000 m above the bottom is taken to be the present reduced-shear region, the mean reduction in current to be 5 cm s^{-1}, and the width of the affected area to be 100 km, which is roughly the size of the current core in DB94. This adjustment procedure produces an extra flux of 5 Sv southward, which, when combined with the additional barotropic flux described above, nearly appears to account for the difference.

Based on this analysis, the strength of the DSO is about half that of previously reported values, much of the difference owing to baroclinic change. Before proceeding, one may ask whether this is at all representative. DB94 claim that the DSO does not vary on timescales longer than a few (1–12) days and that there is no seasonal variability. Here a crude hydrographic view is taken of various timescales for comparison. CONVEX crossed the DSO twice, three days apart, and the north

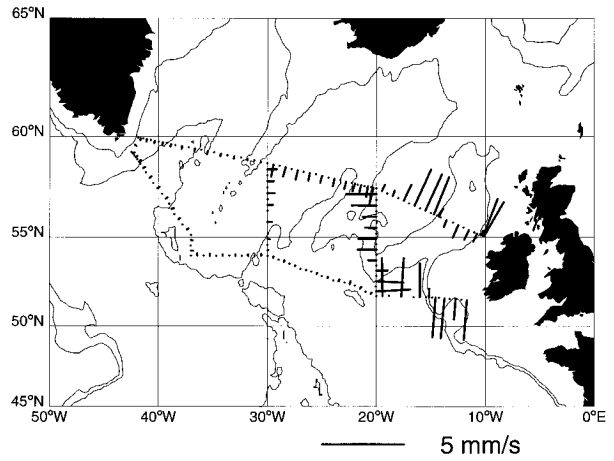

FIG. 10. Solution vector ($\mathbf{m}^{est}$) for five-layer optimal configuration defined by the surface, $\sigma_0 = 27.425$, $\sigma_2 = 36.873$, 36.944, 37.024, and the bottom, with conservation of volume and salt fluxes in all layers, and heat in all but the top layer, for degree 6.

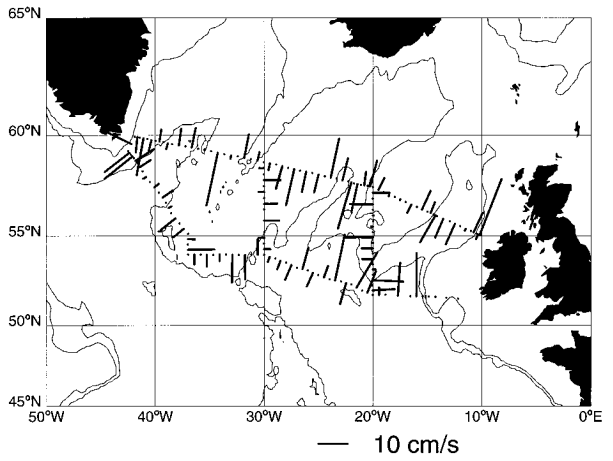

FIG. 11. Offset (ADCP minus geostrophic current) where the geostrophic current is referenced to zero at $\sigma_2 = 36.93$ and the difference is calculated as the mean between 100-m depth and the depth at which ADCP% good is less than 75%. See B94 for further discussion.

section velocity shear profile (not shown) is no different from the south section one (Fig. 4). Next, as kindly provided by R. Hendry (1995, personal communication), data from R/V *Hudson* (WOCE leg AR5) in May 1991 are discussed. Near Greenland, *Hudson* and CONVEX stations were nearly coincident. We inspect changes in baroclinic profiles over the DSO by comparing four station pairs southeastward from the 2000-m isobath: CONVEX 49–50–51–52–53 and *Hudson* 104–105–98–97–96 (see Fig. 2, where *Hudson* positions coincide with respective CONVEX ones). We see from Fig. 12 that the *Hudson* profiles are not much different from CONVEX: The DSO transports less than 2 Sv more in the earlier data than in the later data. It is tempting, therefore, to speculate that the extensive mooring program reported in DB94 concluded just before the start of a significant change in the characteristics of the DSO. Analysis of data post-1991 (elsewhere) should test this hypothesis.

We believe as a result of the foregoing that there is a rationale both for increasing the net southward flow near Greenland and for part of the resulting flow being weaker than would be expected based on previous studies. Now, the application to north and south sections of all conditions in section 3a *except* that of zero net flux results in a near-zero ($<$2 Sv southward) net flux anyway. By imposing an increase on the southward flow, we significantly increase the imbalance (in the appendix, we demonstrate the necessity of forcing the required flux in such a case). Now in constraining the net flux to zero, is it desirable to further constrain the northward balancing flux in terms of location? The answer is *yes.* If the net flux is forced to zero by a constant current correction across both sections, an apparent ''warming'' is caused from the south section to the north because the mean temperature of the north section is higher (by $\sim$1°C) than that of the south section: Proportionally, more of the south section is in the colder subpolar waters than is the north section. The obvious place to force northward flow is where there is already northward flow; in the North Atlantic Current (NAC). The NAC is clearly defined by the high salinity region in the south section from the front in salinity at about 1500 km (Fig. 9) eastward to the continental shelf. Definition of the NAC in the north section is complicated by topography and lateral speading of the salinity signal. However, throughflow in the Rockall Trough, which is a deep cul-de-sac, is not desirable. If northward flow is forced on either flank of the Reykjanes Ridge, then we unbalance the deep circulation, either by amplification of the northward deep current on the west flank, or by causing the disappearance of the southward Iceland–Scotland overflow (ISO) on the east flank. So we narrow down the possible location for the balancing northward flow in the NAC to the east side of the Iceland Basin; particularly the steep western edge of the Rockall–Hatton Plateau. The density structure (Fig. 7) indicates a slope current there, and the ADCP data (Fig. 11) show enhanced currents next to an anticyclonic eddy (roughly stations 25 to 20; also, the presence of the eddy is confirmed by tracers). Thus, there appears to be a northward current at what was the level of no motion in the Labrador Sea Water (LSW). Furthermore, van Aken and de Boer (1995) presented current meter data from the previous year (1990) in nearly the same place and depth range, which show a northeastward current of magnitude about 5 cm s^{-1} (our final preferred circulation scheme, described next, imposes a current of 3 cm s^{-1} over five station pairs: stations 27 to 83).

We believe we have a rationale now for regarding the circulation components of section 3a as generating a minimum (weakest) circulation scheme. It is more difficult to identify similarly a maximum. Nevertheless, we suggest that the foregoing (12.5 Sv increase by

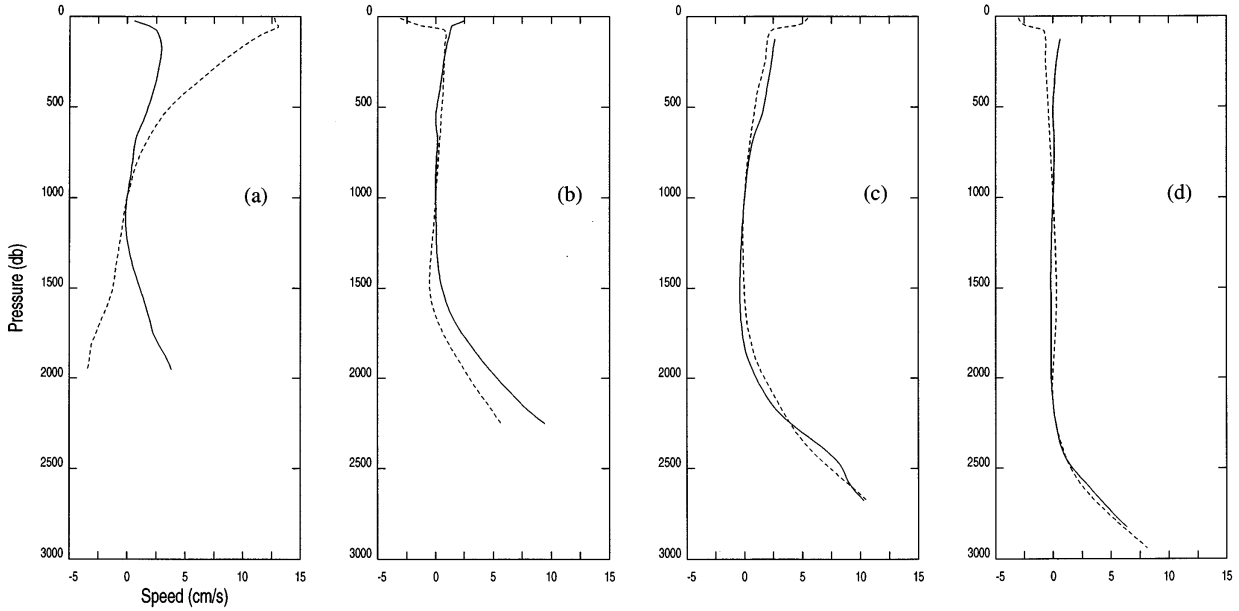

FIG. 12. Comparison of geostrophic profiles referenced to zero at 1000 m for CONVEX (full line) and R/V *Hudson* (faint line), for stations heading offshore from (CONVEX pair first) (a) 49/50 and 104/105, (b) 50/51 and 105/98, (c) 51/52 and 98/97, and (d) 52/53 and 97/96.

Greenland, etc.) is such a maximum because of the inference that the balancing northward flow in the NAC forces too much deep water northward in the Madeira Basin. Therefore, the final preferred state of the circulation in the CONVEX region is intermediate between the minimum and maximum. It has an extra 6.5 Sv forced southward near Greenland (in the last two station pairs of the CONVEX data proper at the western ends of the north and south sections), with the remaining northward flux imbalance in the NAC.

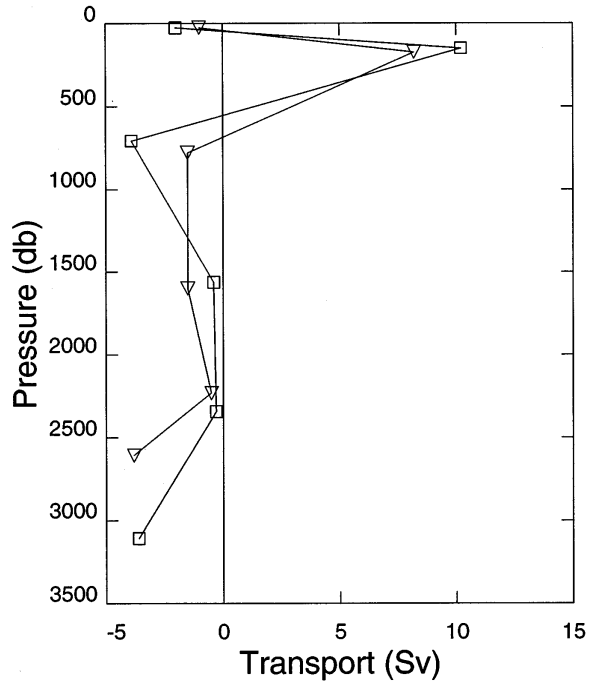

FIG. 13. Horizontally integrated transport for the preferred circulation scheme in the Ekman layer and the five optimal layers; south section is marked by squares, north section by triangles. Pressure axis is constructed from cumulative mean layer thickness.

4. Circulation

The circulation is assembled by considering three parts: upper, from the sum of layers 1 and 2; middepth or LSW from layer 3; and deep, from the sum of layers 4 and 5. Figure 18 shows sketches of each layer's inferred circulation. The net flux balance is 0 Sv, comprised of 7 Sv north (upper), 1 Sv south (LSW), 5 Sv south (deep), and 1 Sv south (Ekman), consistent with horizontally integrated fluxes by layer (Fig. 13).

a. General circulation strength

The strength of the general circulation of the subpolar gyre is deduced from the depth-integrated flux between Cape Farewell and the center of the Irminger Basin, which is the best location for this estimate because the entire (southward) flow, comprising the EGC (the western boundary current) and the DSO (the DWBC), is concentrated there and distinctly separated from the more complicated flows to the south and the east. Reid (1994) placed over 30 Sv there, and Clarke (1984) measured 33.5 Sv, with an alternative of 27 Sv. Schmitz and McCartney's (1993) circulation appears to total 36 Sv (7 Sv greater than 7°C, 14 Sv between 4 and 7°C, 15 Sv below 4°C). Our preferred scheme has 26–27 Sv there with weak and strong alternatives at 20 and 33 Sv.

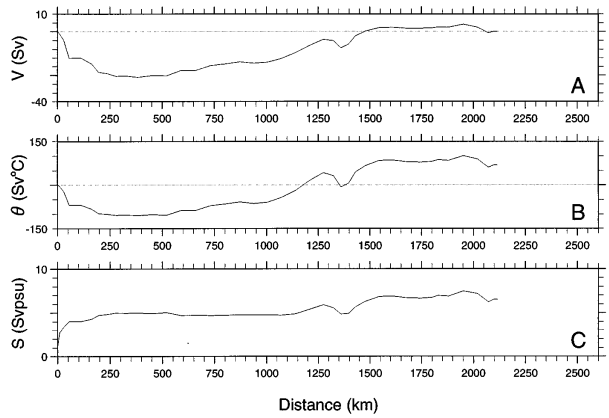

FIG. 14. Depth-integrated transport for the north section, accumulated from zero at the west (left), of (a) volume (V, Sv) and (b) potential temperature (θ, Sv°C); and accumulated from 1.1 Sv psu at the west (see section 2 for an explanation of inshore salt flux), (c) salt (S, Sv psu). Net property flux for the section appears in the easternmost point (the farthest to the right). The faint line is that of zero flux, for reference.

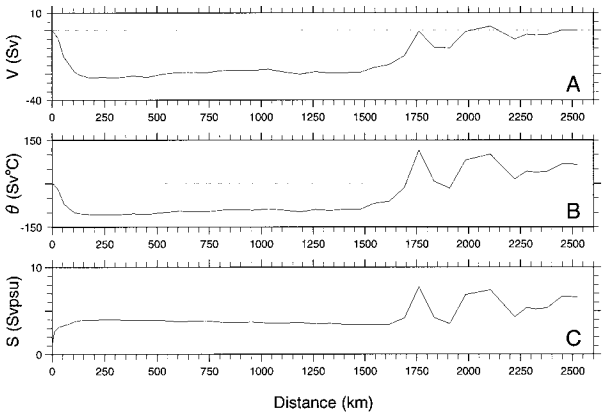

FIG. 15. Depth-integrated transport for the south section, accumulated from zero at the west (left), of (a) volume (V, Sv) and (b) potential temperature (θ, Sv°C); and accumulated from 1.1 Sv psu at the west (see section 2 for explanation of inshore salt flux), (c) salt (S, Sv psu). Net property flux for the section appears in the easternmost point (the farthest to the right). The faint line is that of zero flux, for reference.

The northward flow on the east side of the North Atlantic is noisier (more eddies) and more widespread. On the south section, it is still clearly separated from the southward flow and occurs between about 25°W and the European continental shelf. On the north section it avoids the Rockall Trough and is squeezed onto the west side of the Rockall–Hatton Plateau where the flow is complicated by a large eddy and evidence of recirculation. There are three eddies in the northward flow, all well sampled by the survey, of which two are on the south section and of depth-integrated amplitude 10 and 15 Sv, and a very broad one on the north section of amplitude 10 Sv. All are anticyclonic, and their approximate positions and sizes are shown on the sketch of upper circulation (Fig. 18a).

The total salt flux is divided roughly equally between southward freshwater in the west and northward saline water in the east. Nearly one-third of the total occurs in the westernmost station pair of the EGC, which is shallow (less that 200 m), transports about 1 Sv, and has the most extreme salinity of the section, reaching values less than 30 psu. When the inshore salt flux is included (section 2), 2.7 out of 6.5 Sv psu (over 40% of the section total) are transported on the Greenland shelf, and this is 45% of the inferred freshwater gain of the Arctic.

b. Upper-layer flows

The upper circulation has 18±3 Sv southgoing in the west (see Fig. 18a). The northgoing flow in the south section is subdivided on the salinity front at about 25°W. The flow to the east is called the NAC proper, which has a magnitude of 19 Sv, and the flow to the west, which is weaker and more widespread, is called the recirculation of the subpolar gyre, which has a magni-

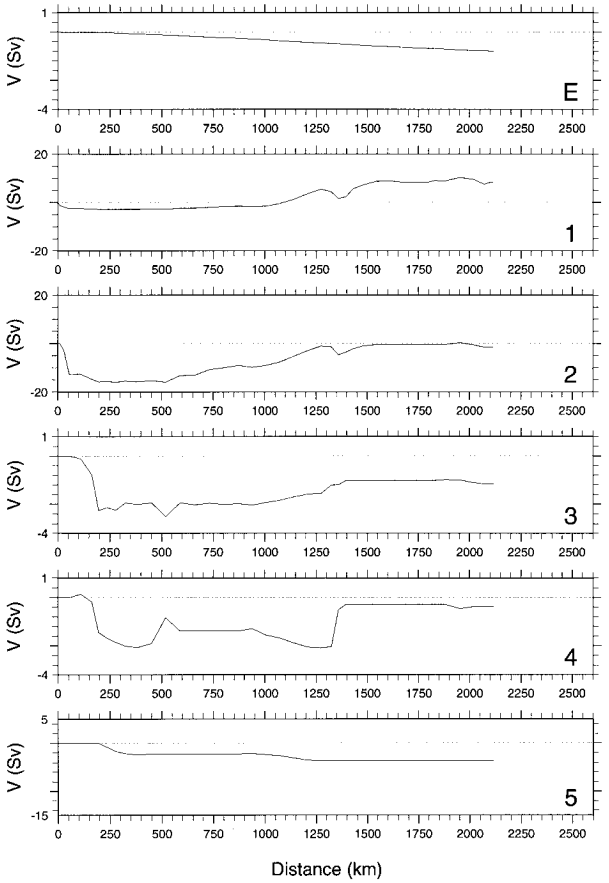

FIG. 16. Volume transport (Sv) for the north section by layer, accumulated from zero at the west (left), where the first panel (e) is the climatological Ekman flux (Sv), and panels 1–5 correspond to each of the five layers in order. Net volume flux for the Ekman flux or the layer appears in the easternmost point (the farthest to the right).

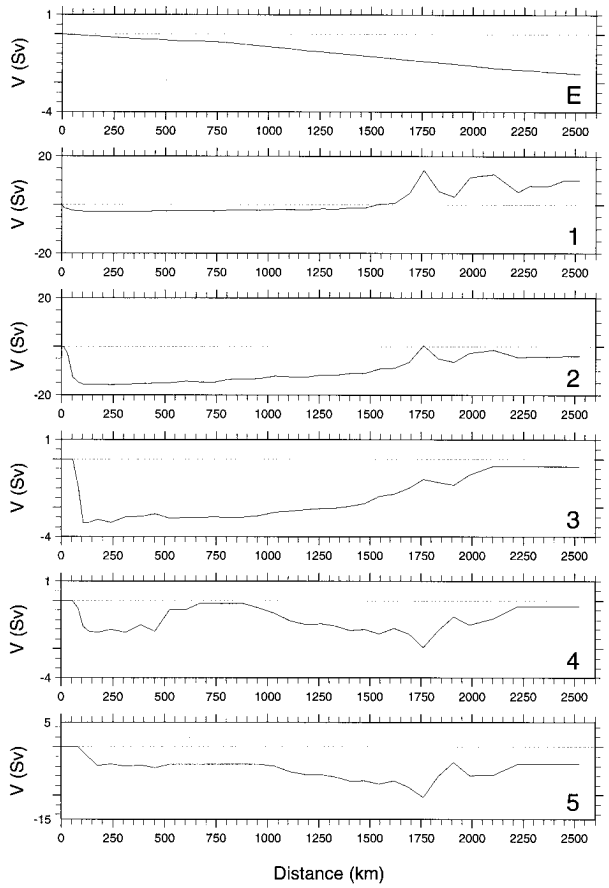

FIG. 17. Volume transport (Sv) for the south section by layer, accumulated from zero at the west (left), where the first panel (e) is the climatological Ekman flux (Sv), and panels 1–5 correspond to each of the 5 layers in order. Net volume flux for the Ekman flux or the layer appears in the easternmost point (the farthest to the right).

tude of 6 Sv. Saunders (1982) had an upper (shallower than 1100 m) transport of 18 Sv northward across 53°N between the European Shelf edge and the MAR, which compares favorably with the above. The upper-layer net flux is 7 Sv northward (which is not affected by barotropic adjustments). The magnitude of the Irminger Current (the northward flow west of the MAR) is estimated at 9 Sv at about 59°N, which compares favorably with the Krauss (1995) estimate of 9.6 Sv at 62°N.

c. Mid-layer (LSW) flows

There is a concentrated southward flow of 3 Sv in the west partially balanced by a very broad northward return flow of 2 Sv east of the MAR (see Fig. 18b). The southward flow is another direct consequence of the addition of the barotropic component to the westernmost two CONVEX pairs on the north and south sections. The presence of the northward flow is supported in general terms by inference from tracers as in Talley and McCartney (1982) and by the analytical study of Cunningham and Haine (1995). The net flow in this layer is 1 Sv southward. The minimum circulation has near-zero fluxes in this layer; the maximum circulation has stronger (5 Sv) southward flow but similar northward return flows.

d. Deep flows

The patterns of the deep flows are well known (e.g., Dickson et al. 1990) (see Fig. 18c). There is the southgoing DSO in the west, supplemented by some of the ISO that, having flowed south down the east side of the MAR, turns in part through the Charlie–Gibbs Fracture Zone, runs north up the west side of the ridge then south along the Greenland shelf edge, and, in overlying the DSO, supplements the DWBC. The DSO transports 5.5 $\pm$ 1.5 Sv: the northward flow on the west flank of the MAR at about 1.5 Sv on both sections, which is reasonable when compared with Saunders' (1994) long-term mean of 2.0 Sv for the Charlie–Gibbs throughflow, and the southward flow on the east flank of the MAR, which is 3 Sv on the north section, 5 Sv on the south section. There is a northgoing input of 4 Sv under the NAC, of which 2 Sv recirculate between the north and south sections to join the ISO, which in turn becomes a flow of 5 Sv of which 1.5 Sv passes through the Charlie–Gibbs Fracture Zone and the remaining 3.5 Sv either recirculates in the eastern basin or flows elsewhere in the western basin. Consequently, 2 Sv are left to flow northward up the west side of the Rockall–Hatton Plateau, which is a large figure, if it all joins the ISO, which is thereby set at only 1 Sv. The net deep flux is 5 Sv southward.

5. Net fluxes

Net fluxes of heat and salt are calculated for zero net volume flux across the north and south sections. The heat flux is calculated according to the method described in Bacon and Fofonoff (1996); an approximate conversion factor from temperature flux to heat flux is found using a mean surface value of specific heat capacity c_p (Gill 1982, Table A3.1) of 3987 J kg^{-1} and a mean in situ density calculated from the data of 1034.5 kg m^{-3} to give 1 PW = 242 Sv°C. There is no apparent significant difference between north and south section fluxes, which for the preferred circulation scheme are 0.28 PW poleward (67 Sv°C) and 6.5 Sv psu poleward. The salinity flux (flux divergence, since we set net volume flux to zero) equates either to a southward freshwater flux of 0.19 Sv (0.19×10^9 kg s^{-1}) or to a northward salt flux of 6.5×10^6 kg s^{-1}.

Next, the estimation of net flux errors is described. We separated the errors into ''inverse'' and ''oceanographic'' and subjected the two categories to sensitivity testing. The sensitivity to variations in the inverse model were arrived at by making six different models, a ''basic'' one (constrained as in section 3a), a ''simple'' one (net flux constraint only), and four others that (a)

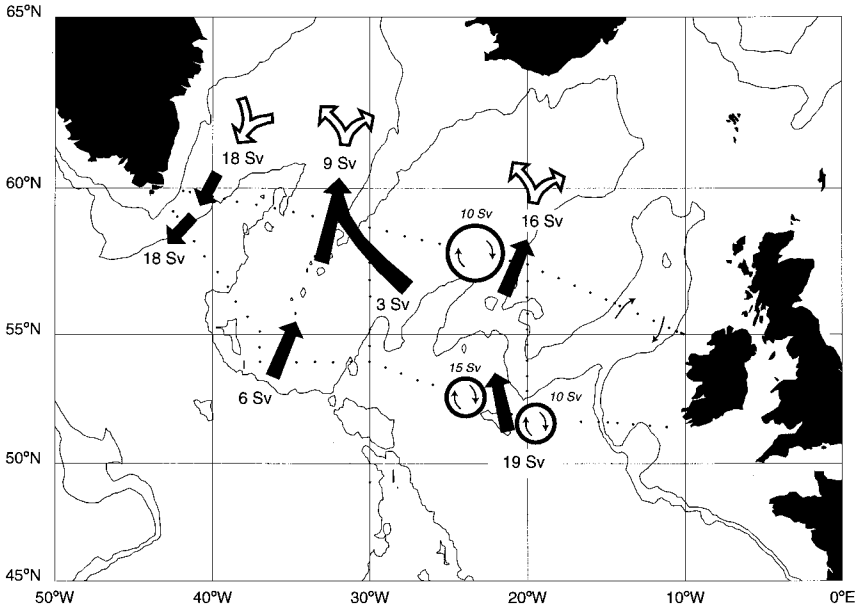

FIG. 18a. Upper circulation sketch, formed from the sum of layers 1 and 2. The rings show approximate sizes, positions, and rotational senses of eddies, whose magnitude is given in small italic type. The filled arrows show approximate locations and directions of currents whose magnitude is given in large type. The NAC in the east is broad to the south and narrow to the north. A small amount joins the ''central'' recirculation, which is a broad flow filling the region between the western currents and the NAC. Unquantified senses of currents are given north of the CONVEX region (unfilled arrows) and in the Rockall Trough (small arrows), where there is a weak recirculation (probably 1–2 Sv).

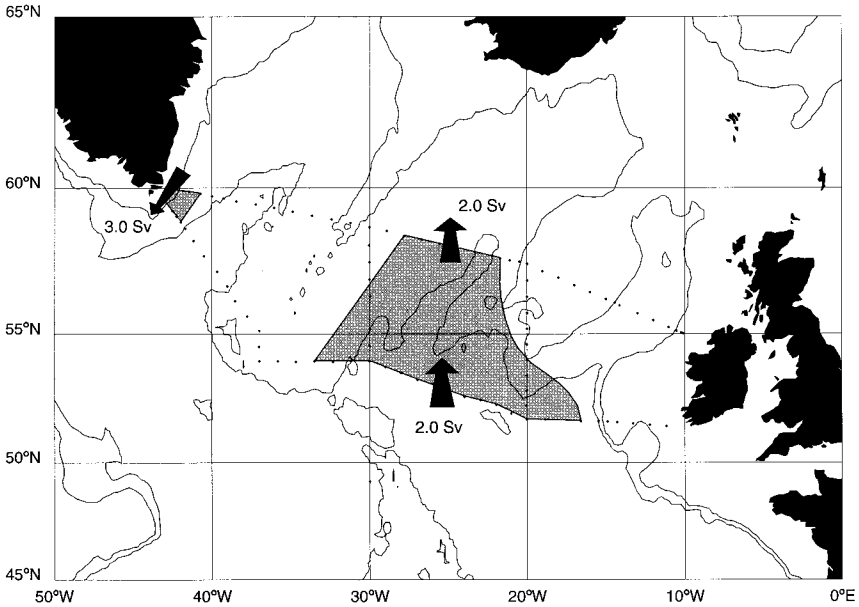

FIG. 18b. Middepth (LSW) circulation (layer 3). The approximate lateral extent of the regions of measurable flow is shown shaded. Arrows show flow direction, and associated magnitude is indicated.

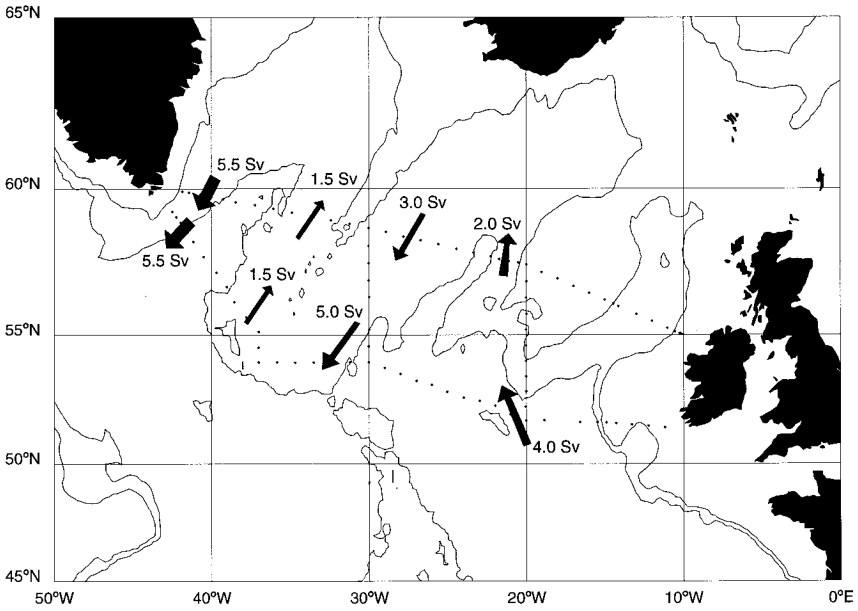

FIG. 18c. Deep circulation sketch, formed from the sum of layers 4 and 5. The Denmark Strait overflow is shown to the west by Greenland. The 1.5 Sv on the west flank of the Reykjanes Ridge is assumed to have passed through the Charlie–Gibbs Fracture Zone. In the north Madeira Basin and Iceland Basin, half of the northgoing 4 Sv appears to recirculate between the north and south sections, and half north of the CONVEX region. This is supplemented by 1 Sv of Iceland–Scotland overflow on the east flank of the ridge.

changed the basic model's initial level of no motion, (b) changed the basic model's layers from the optimal set to a pseudorandom set, (c) changed the basic model's constraints to exact volume flux conservation only, and (d) changed model (a)'s solution degree. Thus, with six solutions on the two sections, the computed standard error of the 12 solutions is shown as the first line in Table 1.

The oceanographic variations (Table 1) were computed as follows. A range of ±25% was allowed in the strength of the Ekman flux, approximately the size of the annual cycle, from which no salinity error results because the mean Ekman salinity is the nearly the same as the section mean salinity. The errors due to our EGC were estimated by allowing ± 6 cm s^{-1} in the computed reference currents, taking into consideration that the standard deviation of the ADCP estimates was 12 cm s^{-1} and the standard error of the mean 1 cm s^{-1}. The circulation range is computed from the extremes described in section 3. The EGC inshore salt flux error is described in section 2. Thus, the net fluxes are 0.28 ± 0.06 PW and 6.5 ± 2.2 Sv psu. The heat flux estimate is not significantly different from that for 55°N in Isemer et al. (1989), which in turn is little changed from Bunker (1976) and a little lower than that in Trenberth and Solomon (1994), 0.35 PW.

TABLE 1. Net flux errors. Salt flux error (S error, Sv psu) and potential temperature flux error ($\boldsymbol{\theta}$ error, Sv°C) are presented for the oceanographic and inverse sensitivity tests. North and south section statistics are conflated, as no significant difference was found between sections.

Condition	$\boldsymbol{\theta}$ error (Sv°C)	S error (Sv psu)
Inverse sensitivity tests	5.1	0.41
Oceanographic sensitivity tests:		
(i) EGC	1.6	0.43
(ii) Ekman	1.6	0.00
(iii) Circulation extremes (section 3)	6.0	0.39
EGC inshore salt flux	—	1.00
Total error (total flux)	14.3 (67.0)	2.23 (6.5)
Total (%)	21%	34%

The present results are compared with those of McCartney and Talley (1984). They have a three-box model (their Fig. 5); only two of these, representing upper and lower layers in the subpolar North Atlantic, south of the Greenland–Scotland Ridge and north of 50°N are of interest here. From the temperature and volume flux values in their Table 2, we calculate values of the net temperature flux across 50°N, which fall into two groups: one 128 (±1) Sv°C (their basic setup) and the other 159 Sv°C, forced with a high ocean–atmosphere heat flux in the Norwegian Sea. Then in their box model, the difference between the CONVEX fluxes (taken as representative of conditions at the north ends of their two southern boxes) and their 50°N fluxes is given by the heat lost by the ocean to the atmosphere over the subpolar North Atlantic (their Q_{SPNA}), for which they quote an unpublished value due to Bunker of 87 Sv°C. Thus, values of about 40 and 72 Sv°C (0.17 and 0.30

PW) are found for their net heat flux across the CONVEX region, which, when compared with the CONVEX heat flux of 0.28 PW, implies that the high ocean–atmosphere heat flux case is appropriate here.

6. Arctic freshwater flux

Now that the salt flux between Cape Farewell and Ireland has been estimated, the freshwater budget of the Arctic basin will be examined next, and comments will be made on the estimates of Aagaard and Carmack (1989, hereafter AC89). Following AC89, the significant elements in the budget are identified. These are (i) the Bering Strait inflow T_B (0.8 Sv, ±25%) at salinity S_B (32.5 psu); (ii) Atlantic (south section) net flux T_A at salinity S_A (34.956 psu), where T_A is unknown; (iii) Atlantic (south section) salt flux C (6.5 ± 1.6 Sv psu) for zero net volume flux; (iv) Canadian Archipelago throughflow, T_C at salinity S_C, discussed below; (v) ice export through the Denmark Strait I; and (vi) Arctic freshwater input F. Then the volume flux (1) and salt flux (2) can be written as:

$$T_A + T_B + T_C + I + F = 0 \tag{1}$$

$$S_A T_A + S_B T_B + S_C T_C + C = 0. \tag{2}$$

Considering the Canadian Archipelago thoughflow, we use the Fissel et al. (1988) transport of 1.7 Sv south with the Aagaard and Greisman (1975) mean salinity of 34.2 psu (in the same way as AC89). Ice export in the EGC is estimated by taking the value reported in AC89 for export through the Denmark Strait (560 km^3 yr^{-1}, or 0.018 Sv), and then estimating the reduction in width between Denmark Strait and Cape Farewell of the East Greenland ice extent from Gloersen et al. (1992); this is about 40% on an annual basis, leaving ice export off Cape Farewell about 0.007 Sv.

From these we obtain a freshwater gain for the Arctic of 0.17 Sv, and a net northward flux across the CONVEX region of 0.73 Sv. If the Canadian Archipelago throughflow is suspected to be too high, then performing the calculation again but with $T_C = 0$ reduces the freshwater gain to 0.14 Sv and reverses the mean Atlantic flux (T_A is 0.97 Sv southward), so overestimating T_C biases the freshwater gain high.

From AC89, the Arctic freshwater gain may be calculated both by oceanic budgeting (as above) and by their direct estimation of evaporation, precipitation, etc. The former results in a gain of 0.11 Sv (Bering Strait input, Canadian Archipelago export, Denmark Strait ice export, Atlantic water exchange); the latter in a gain of 0.20 Sv (Arctic and GIN sea precipitation minus evaporation, and runoff, and input from the Skaggerak). The direct estimate is similar to that obtained from Baumgartner and Reichel (1975); integrating their data from the Bering Strait to 55°N in the Atlantic, a gain of 0.22 Sv is found. Thus, the present estimate of Arctic freshwater gain (0.17 Sv, depending principally on the estimates for T_B and T_C) tends toward a value closer to AC89's direct than indirect estimates. The calculation is controlled mainly by C and T_B because S_C is not too dissimilar from S_A. The total error of our estimate is about 35%: 0.17 ± 0.06 Sv.

7. Conclusions

We have calculated the heat and salinity fluxes across the CONVEX region as 0.28 ± 0.06 PW and 6.5 ± 2.2 Sv psu, and the net freshwater gain of the Arctic as 0.17 ± 0.06 Sv. A circulation scheme has been presented for the CONVEX region, most elements of which agree with previous observations and estimates, with the notable exception of the Denmark Strait overflow, the strength of which is about half of that expected.

Acknowledgments. Thanks are due to the officers and crew of the RRS *Charles Darwin* for their assistance. The quality of the CTD data was assured by Peter Saunders, Jane Read, John Gould, Pat Gwilliam (IOSDL), Mark Brandon (SPRI), and Chris Paulson (RVS). Particular thanks are due to Harry Bryden and Peter Saunders for advice and assistance and to the referees for their helpful criticism.

APPENDIX

Arbitrary Adjustment of Matched Inflow and Outflow

Consider a case, like the western end of CONVEX, where an inflow to a box may be very closely matched (in topographic characteristics and orientation, and in property characteristics) by an outflow. A box inverse has no skill in determining large barotropic current components in this case. With solution vector $\mathbf{m}$, data vector $\mathbf{d}$, and geometry matrix $\mathbf{G}$, the SVD imposes the usual conditions of min $\|\mathbf{m}\|$ and min $\|\epsilon\|$, where $\varepsilon = \mathbf{G}\,\mathbf{m} - \mathbf{d}$, the error vector. The change in square length caused by adding an arbitrary outflow $(+b)$ to element k of $\mathbf{m}$, matched by the same inflow $(-b)$ to element l of $\mathbf{m}$ is detailed as follows:

$$\begin{aligned} m_k' &= m_k + b, \\ m_l' &= m_l - b. \end{aligned} \tag{A1}$$

Then the difference in square lengths of $\mathbf{m}'$ and $\mathbf{m}$ is

$$\begin{aligned} \|\mathbf{m}'\|^2 - \|\mathbf{m}\|^2 &= \mathbf{m}'^{\mathrm{T}}\mathbf{m}' - \mathbf{m}^{\mathrm{T}}\mathbf{m} \\ &= (m_k + b)^2 + (m_l - b)^2 - m_k^2 - m_l^2 \\ &= 2b^2 \end{aligned} \tag{A2}$$

if $m_k, = m_l$. Plainly the solution length is increased by this action; however, the solution error is not. Pursuing the same logic, consider layer (constraint) i, an element of ε:

$$\epsilon_i = \sum_j G_{ij} m_j - d_i, \tag{A3}$$

summing over columns of G labeled j. Ignoring all elements except k and l, which are redefined as before:

$$\begin{aligned}\epsilon_i' &= G_{ik}(m_k + b) + G_{il}(m_l - b) - d_i \\ &= G_{ik}m_k + G_{il}m_1 - d_i \\ &= \epsilon_i; \end{aligned} \tag{A4}$$

if $G_{ik} = G_{il}$, areas and property distributions are the same. Thus, the solution length constraint (but not the error constraint) holds the solution length from increasing and, if the value of b is not known a priori in these circumstances (by current meters, ADCP, floats, etc.), the box inverse method will not predict it.

REFERENCES

Aagaard, K., and P. Greisman, 1975: Toward new mass and heat budgets for the Arctic Ocean. *J. Geophys. Res.,* **80,** 3821–3827.

——, and E. C. Carmack, 1989: The role of sea ice and other fresh water in the Arctic circulation. *J. Geophys. Res.,* **94,** 14 485–14 498.

Bacon, S., 1994: Skill in an inversion solution: CONVEX-91 hydrographic results compared with ADCP measurements. *J. Atmos. Oceanic Technol.,* **11,** 1569–1591.

——, and N. P. Fofonoff, 1996: Oceanic heat flux calculation. *J. Atmos. Oceanic Technol.,* **13,** 1327–1329.

Baumgartner, A., and E. Reichel, 1975: *The World Water Balance.* Elsevier, 179 pp.

Bryden, H. L., and M. M. Hall, 1980: Heat transport across 25°N latitude in the Atlantic Ocean. *Science,* **207,** 884–886.

Bunker, A., 1976: Computations of surface energy flux and annual air–sea interaction cycles of the North Atlantic Ocean. *Mon. Wea. Rev.,* **104,** 1122–1140.

Clarke, R. A., 1984: Transport through the Cape Farewell-Flemish Cap section. *Rapp. P.-V. Réun. Cons. Int. Explor. Mer,* **185,** 120–130.

Coachman, L. K., and K. Aagaard, 1989: Transports through Bering Strait: Annual and interannual variability. *J. Geophys. Res.,* **93,** 15 535–15 539.

Cunningham, S. A., and T. W. N. Haine, 1995: Labrador Sea water in the eastern North Atlantic. Part I: A synoptic circulation inferred from a minimum in potential vorticity. *J. Phys. Oceanogr.,* **25,** 649–665.

Dickson, R. R., and J. Brown, 1994: The production of North Atlantic Deep Water: Sources, rates and pathways. *J. Geophys. Res.,* **99** (C6), 12 319–12 341.

——, E. M. Gmitrowicz, and A. J. Watson, 1990: Deep-water renewal in the northern North Atlantic. *Nature,* **344,** 848–850.

Dietrich, G., 1969: *Atlas of the Hydrography of the Northern North Atlantic Ocean, Based on the Polar Front Survey of the International Geophysical Year, Winter and Summer 1958.* Conseil International pour l'Exploration de la Mer, 140 pp.

Fissel, D. B., D. D. Lemon, H. Melling, and R. A. Lake, 1988: Nontidal flows in the North-West Passage. Canadian Tech. Rep. Hydrography Ocean Sciences 98, 143 pp. [Available from Institute of Ocean Sciences, Sidney BC V8L 4B2, Canada.]

Gill, A. E., 1982: *Atmosphere–Ocean Dynamics.* Academic Press, 662 pp.

Gloersen, P., W. J. Campbell, D. J. Cavalieri, J. C. Comiso, C. L. Parkinson, and H. J. Zwally, 1992: *Arctic and Antarctic Sea Ice 1978–1987: Satellite Passive-Microwave Observations and Analysis.* National Aeronautics and Space Administration, 290 pp.

Gould, W. J., 1992: RRS *Charles Darwin* Cruise 62 1 August–4 September 1991. CONVEX - WOCE Control Volume AR12. IOSDL Cruise Report No. 230, Wormley, 60 pp. [Available from National Oceanographic Library, Southampton Oceanography Centre, Empress Dock, Southampton SO14 3ZH, United Kingdom.]

Hellerman, S., and M. Rosenstein, 1983: Normal monthly wind stress over the world ocean with error estimates. *J. Phys. Oceanogr.,* **13,** 1093–1104.

Isemer, H.-J., J. Willebrand, and L. Hasse, 1989: Fine adjustment of large-scale air–sea energy flux parameterisations by direct estimates of ocean heat transport. *J. Climate,* **2,** 1173–1184.

Krauss, W., 1995: Currents and mixing in the the Irminger Sea and in the Iceland Basin. *J. Geophys. Res.,* **100** (C6), 10 851–10 871.

McCartney, M. S., and L. D. Talley, 1984: Warm-to-cold water conversion in the northern North Atlantic Ocean. *J. Phys. Oceanogr.,* **14,** 922–935.

Read, J. F., and W. J. Gould, 1992: Cooling and freshening of the subpolar North Atlantic Ocean since the 1960s. *Nature,* **360** (6399), 55–57.

Reid, J. L., 1994: On the total geostrophic circulation of the North Atlantic Ocean: Flow patterns, tracers, and transports. *Progress in Oceanography,* Vol. 33, Pergamon Press, 1–92.

Roach, A. T., K. Aagaard, C. H. Pease, S. A. Salo, T. Weingartner, V. Pavlov, and M. Kulakov, 1995: Direct measurements of transport and water properties through the Bering Strait. *J. Geophys. Res.,* **100**(C9), 18 443–18 457.

Saunders, P. M., 1982: Circulation in the eastern North Atlantic. *J. Mar. Res.,* **40**(Suppl.), 641–657.

——, 1994: The flux of overflow water through the Charlie-Gibbs Fracture Zone. *J. Geophys. Res.,* **99**(C6), 12 343–12 355.

Schmitz, W. J., and M. S. McCartney, 1993: On the North Atlantic circulation. *Rev. Geophys.,* **31,** 29–49.

Talley, L. D., and M. S. McCartney, 1982: Distribution and circulation of Labrador Sea water. *J. Phys. Oceanogr.,* **12,** 1189–1205.

Trenberth, K. E., and A. Solomon, 1994: The global heat balance: Heat transports in the atmosphere and ocean. *Climate Dyn.,* **10**(3), 107–134.

van Aken, H. M., and C. J. de Boer, 1995: On the synoptic hydrography of intermediate and deep water masses in the Iceland Basin. *Deep-Sea Res.,* **42** (2), 165–189.

Wunsch, C., 1978: The North Atlantic circulation west of 50°W determined by inverse methods. *Rev. Geophys.,* **16,** 583–620.